Study of the phase transitions by observation of the A and ^{1}H nuclear magnetic resonance in ANH_4SO_4 (A = ^{7}Li, ^{39}K and ^{87}Rb) single crystals with excellent optical quality

2008 J. Phys.: Condens. Matter 20 335201

(http://iopscience.iop.org/0953-8984/20/33/335201)

J. Phys.: Condens. Matter **20** (2008) 335201 (7pp) doi:10.1088/0953-8984/20/33/335201

Study of the phase transitions by observation of the A and ^{1}H nuclear magnetic resonance in ANH_4SO_4 (A = ^{7}Li, ^{39}K and ^{87}Rb) single crystals with excellent optical quality

Ae Ran Lim[1,3] **and Sun Ha Kim**[2]

[1] Department of Science Education, Jeonju University, Jeonju 560-759, Korea
[2] Solid State Analysis Team, Korea Basic Science Institute, Daegu 702-701, Korea

E-mail: aeranlim@hanmail.net and arlim@jj.ac.kr

Received 12 March 2008, in final form 2 July 2008
Published 21 July 2008
Online at stacks.iop.org/JPhysCM/20/335201

Abstract

ANH_4SO_4 (A = Li, K and Rb) single crystals were grown using the slow evaporation method. We studied the spectra, spin–lattice relaxation times, T_1, and spin–spin relaxation times, T_2, of the ^{1}H, ^{7}Li, ^{39}K and ^{87}Rb nuclei in these three types of single crystals. The nuclear magnetic resonance observations provided a consistent description of the dynamics of the studied nuclei in these materials. The T_1 values for the ^{1}H nuclei are similar in all three crystals and the ^{1}H spin–lattice relaxation times increase with increasing temperature. However, as the radii of the metal ions increase, a corresponding decrease in the spin–lattice relaxation times of the A nuclei is observed. The differences observed in the spin–lattice relaxation times of the A nuclei upon changing the alkali-metal ion may be related to the ionic radius and the lengths of the A–O bonds. Therefore, the occurrence of phase transitions in these materials seems to be essentially dependent on the presence of the metal ions.

1. Introduction

The increasing number of reports on the physical properties of ANH_4SO_4 systems (where A represents the alkali-metal ion Li, K and Rb) is largely attributed to the excellent optical properties of single crystals of these complex sulfate compounds [1–3]. The structures of these materials are based on the AO_4 tetrahedron, that is, the alkali-metal ion is surrounded by tetrahedrally coordinated oxygen species. In particular, $LiNH_4SO_4$ single crystals undergo several phase transitions below and above room temperature. The phases of $LiNH_4SO_4$ are as follows: phase I from the melting point to 459.5 K; phase II from 459.5 to 284.5 K; phase III from 284.5 to 27 K; and phase IV below 27 K [4–6]. Phase I has an orthorhombic structure characterized by the unit-cell parameters $a = 5.13$ Å, $b = 5.16$ Å and $c = 8.74$ Å [7]; phase II exhibits similar unit-cell parameters as those of phase I [8]; phase III has a monoclinic structure [4, 9]; and finally, phase IV has a monoclinic unit cell [10–12]. Moreover, Watton *et al* [13] reported a new phase transition for this compound (at 133 K), in addition to those previously observed at 27, 284.5 and 459.5 K. On the other hand, KNH_4SO_4 crystals do not exhibit any phase transitions. KNH_4SO_4 is known to be orthorhombic with space group *Pmcn*. Its unit-cell dimensions are $a = 5.8$ Å, $b = 10.1$ Å, $c = 7.5$ Å and $Z = 4$ [14]; however, no detailed crystal structure has been reported for this compound. In the $RbNH_4SO_4$ crystals, the phase-transition temperatures are 120 and 189 K [15, 16]. The structure of an $RbNH_4SO_4$ crystal at room temperature was found to be orthorhombic, with the space group *Pnma* and the unit-cell dimensions: $a = 7.8303$ Å, $b = 5.9772$ Å, $c = 10.4677$ Å and $Z = 4$ [17]. No detailed information about the structural characteristics of this crystal is available in the literature. The

[3] Author to whom any correspondence should be addressed.

Table 1. The structure, space group, lattice constants and bond length in the ANH_4SO_4 (A = Li, K and Rb) single crystals at room temperature.

	$LiNH_4SO_4$	KNH_4SO_4	$RbNH_4SO_4$
Structure	Orthorhombic	Orthorhombic	Orthorhombic
Space group	*Pmnn*	*Pmcn*	*Pnma*
Lattice constants	$a = 5.28$ Å	$a = 5.8$ Å	$a = 7.8303$ Å
	$b = 9.14$ Å	$b = 10.1$ Å	$b = 5.9772$ Å
	$c = 8.786$ Å	$c = 7.5$ Å	$c = 10.4677$ Å
Bond length (A–O)	1.914 Å		2.867 Å
Phase-transition temperature	$T_{C1} = 459.5$ K		$T_{C1} = 189$ K
	$T_{C2} = 284.5$ K		$T_{C2} = 120$ K
	$T_{C3} = 133$ K		
	$T_{C4} = 27$ K		

structure, space group, lattice constants and bond length of the AO_4 tetrahedra in ANH_4SO_4 (A = Li, K or Rb) single crystals are summarized in table 1.

In this paper, we discuss the temperature dependences of the spectra, the spin–lattice relaxation times, T_1, and the spin–spin relaxation times, T_2, for the A and ^{1}H nuclei in single crystals of ANH_4SO_4 (A = Li, K and Rb), with particular emphasis on the role of the relaxation times on the pre-transitional effects. These observations of the nuclear magnetic resonance (NMR) of the ^{1}H, ^{7}Li, ^{39}K and ^{87}Rb nuclei in single crystals of $LiNH_4SO_4$, KNH_4SO_4 and $RbNH_4SO_4$ are used to obtain information about their structural phase transitions. Here, we compare the results obtained for the three studied ANH_4SO_4 crystals, which all have similar sulfate structures, and discuss the effect of the ionic radius of the alkali-metal ions on the phase transition in each crystal. We are particularly interested in understanding the role of the alkali-metal ions in the structural phase transitions in these compounds.

2. Experimental methods

Single crystals of ANH_4SO_4 (A = Li, K and Rb), with good optical properties, were grown at room temperature by means of the slow evaporation method from a saturated aqueous solution containing A_2SO_4 and $(NH_4)_2SO_4$. The obtained crystals were colorless and transparent. The $LiNH_4SO_4$ crystals had the shape of a parallelepiped, whereas the KNH_4SO_4 and $RbNH_4SO_4$ crystals exhibited hexagonal shapes.

The NMR signals of the A and ^{1}H nuclei in the ANH_4SO_4 (A = Li, K and Rb) single crystals were measured using the Varian 200 FT NMR and Bruker 400 FT NMR spectrometers at the Korea Basic Science Institute. The static magnetic fields used were 4.7 and 9.4 T, respectively, and the central radio frequency was set at $\omega_o/2\pi = 200.13$ MHz for the ^{1}H nuclei, at $\omega_o/2\pi = 155.51$ MHz for the ^{7}Li nuclei, at $\omega_o/2\pi = 18.67$ MHz for the ^{39}K nuclei and at $\omega_o/2\pi = 130.93$ MHz for the ^{87}Rb nuclei. For the T_1 measurements, a π–t–$\pi/2$ inversion recovery pulse sequence was used in the ^{1}H and ^{7}Li experiments, whereas a $\pi/2$–t–$\pi/2$ saturation recovery pulse sequence was used in the ^{39}K and ^{87}Rb experiments. The width of the π pulse was 3 μs for ^{1}H, 33.3 μs for ^{39}K, 5 μs for ^{7}Li and ^{87}Rb. In addition, the spin–spin relaxation time, T_2, was determined using a $\pi/2$–t–π pulse sequence with the spin echo method. The sample temperatures were maintained at constant values by controlling the flow of helium gas and the heater current, thereby giving an accuracy of $\pm 0.5\,^\circ$C.

3. Experimental results and analysis

^{1}H spin–spin relaxation times were obtained for single crystals of $LiNH_4SO_4$, KNH_4SO_4 and $RbNH_4SO_4$. The inversion recovery traces of the ^{1}H ($I = 1/2$) nuclei can each be represented by a single exponential function. The ^{1}H spin–lattice relaxation times were determined by fitting the recovery patterns to the following equation [18]:

$$[S(\infty) - S(t)]/2S(\infty) = \exp(-Wt), \tag{1}$$

where $S(t)$ is the nuclear magnetization at time t and W is the transition probability corresponding to $\Delta m = \pm 1$. The relaxation time is given by $T_1 = 1/W$.

The saturation recovery traces for the central lines of ^{7}Li, ^{39}K and ^{87}Rb ($I = 3/2$), with dominant quadrupole relaxation in $LiNH_4SO_4$, KNH_4SO_4 and $RbNH_4SO_4$, can be represented by the following combination of two exponential functions [19, 20]:

$$[S(\infty) - S(t)]/S(\infty) = 0.5[\exp(-2W_1t) + \exp(-2W_2t)]. \tag{2}$$

Here

$$W_n = K_n \int_{-1}^{1} (1 - p^2) W(p) \frac{\tau_c(p)}{1 + [n\omega_L \tau_c(p)]^2}\, \mathrm{d}p, \quad n = 1, 2, \tag{3}$$

where W_1 and W_2 ($n = 1, 2$) designate the ^{7}Li, ^{39}K and ^{87}Rb spin–lattice transition rates corresponding to the transitions $\Delta m = \pm 1$ and $\Delta m = \pm 2$, respectively, and $S(t)$ is the nuclear magnetization corresponding to the central transition at time t after saturation. The spin–lattice relaxation time is given by [20]

$$1/T_1 = \tfrac{2}{5}(W_1 + 4W_2). \tag{4}$$

3.1. ^{1}H and ^{7}Li NMR in $LiNH_4SO_4$ crystals

The ^{1}H spin–lattice relaxation time was measured between 6 and 280 K at a frequency of 200.13 MHz. The proton spin–lattice relaxation time was measured using a inversion recovery pulse sequence in the whole studied temperature range. The relaxation time, T_1, presented in equation (1) was determined directly from the slope of a plot of the log $[S(\infty) - S(t)]/2S(\infty)$ versus time (t). The spin–lattice relaxation patterns can be described quite well by a single exponential form at all temperatures. The values of T_1 measured below 280 K are given as a function of $1000/T$ in figure 1. The changes in the T_1 curve observed at temperatures close to T_{C3} (=133 K) and T_{C4} (=26 K) correspond to phase transitions. The relaxation time increases with temperature in phases IV and III, although the rate is slightly slower in phase IV. In phase III′, the variation of T_1 with temperature exhibits a maximum; T_1 slowly increases as the temperature is increased and then

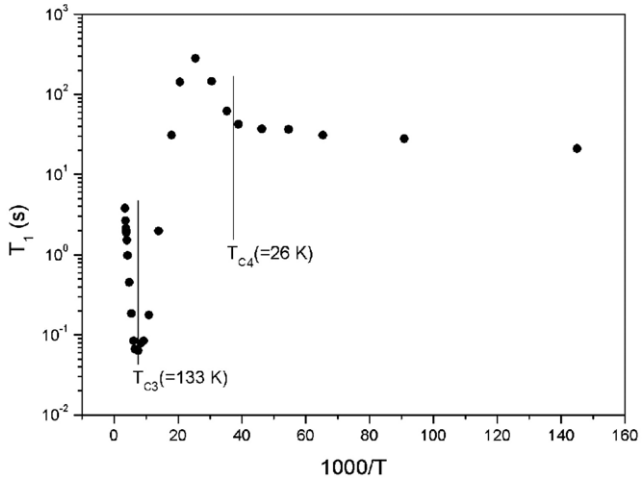

Figure 1. Temperature dependence of the spin–lattice relaxation time, T_1, for ^{1}H in $LiNH_4SO_4$ crystals.

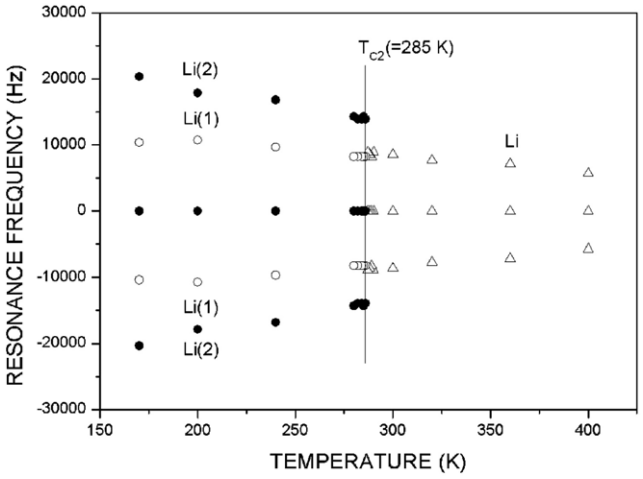

Figure 2. Splitting of the Li(1) and Li(2) resonance lines in $LiNH_4SO_4$ crystals as a function of the temperature.

begins to decrease after passing through a maximum. This trend is similar to that reported by Shenoy *et al* [21]. Then, in phases III and IV, T_1 undergoes fast motions, whereas in phase III′ the motion is much slower. The spin–lattice relaxation time is short at 133 K, that is, $T_1 = 63.5$ ms, and very long at 26 K, namely, $T_1 = 42\,400$ ms. The T_1 values can be related to corresponding values of the rotational correlation time, τ_c, which is the time a molecule remains in a given state before reorienting [22]. Activation energies for the reorientational motion in all phases can be obtained from curves of the correlation time versus $1000/T$. The activation energies in phases III and IV were determined to be 2.61 kcal mol^{-1} and 12.39 cal mol^{-1}, respectively. In phase III′, T_1 increases with temperature to a maximum point at 39 K, while those above 39 K are decreased. The E_a of 1.23 kcal mol^{-1} obtained from our experimental results [23] in phase III′ is consistent with the results reported by Watton *et al* [13]. The trend observed for T_1 below 133 K is similar to that reported for phase III by Shenoy *et al* [21]. Our observed changes in the activation energy are consistent with the results obtained for the T_1 of ^{1}H by Watton *et al* [13] and Shenoy *et al* [21]. At temperatures below 27 K, the activation energy has a value smaller than 12.39 cal mol^{-1}. The large activation energy observed in phase III indicates that the NH_4 groups are significantly affected during this transition.

The ^{7}Li NMR spectra were measured in the temperature range between 170 and 400 K (see figure 2). Here, the magnetic field was applied at 10° from the *a* axis in the *ac* plane. Such a spectrum consists of only three lines for all orientations of the crystal above T_{C2} (=285 K). This three-line structure is a result of the quadrupole interactions of the ^{7}Li nucleus. Two different Li resonance groups were recorded in phase III, originating from Li(1) and Li(2). These two signals are associated with two physically inequivalent positions of the Li atoms in the unit cell. The phase transition at 285 K coincided with a change in the splitting of the Li resonance line associated with the breaking of local symmetry at the Li site. The changes in the line positions indicate that the electric field gradients (EFG) at the Li sites change with temperature, which in turn means that the neighboring atoms of Li are displaced from their high-temperature positions. To measure the spin–lattice relaxation time, T_1, for ^{7}Li, a π–t–$\pi/2$ pulse sequence was applied at 54.7° from the *c* axis in the *ac* plane of the crystal. The resonance spectrum in this direction consists of a single resonance line instead of three resonance lines for Li. The nuclear magnetization $S(t)$ of ^{7}Li at time t after the π pulse was determined from the inversion recovery sequence following the pulse. The relaxation time T_1 in equation (1) was determined directly from the slope of a plot of $\log[S(\infty) - S(t)]/S(\infty)$ versus time (t). This trace can be well described by a single exponential function. The temperature dependence of T_1 for ^{7}Li in the single crystal is shown in figure 3. The spin–lattice relaxation time is very long, namely, $T_1 = 550$ s at 300 K. The discontinuities observed in the T_1 curve near 285 K correspond to a phase transition from the orthorhombic to the monoclinic structure, which means that the phase III to phase II transition is a first-order transition. The relaxation time increases with temperature in both phases, although it is slightly slower in phase II. The activation energies in phases III and II were determined to be 2.61 and 0.88 kcal mol^{-1}, respectively. Our observed changes in the activation energy are consistent with the values obtained by Shenoy and Ramakrishna for ^{1}H from studies of the relaxation times [21]. The large change in the activation energy observed at 285 K indicates that the LiO_4 groups are significantly affected during this transition [24]. The changes in the geometry of the oxygen atoms from the sulfate groups around the Li nucleus play an important role in the phase transition.

3.2. *^{1}H and ^{39}K NMR in KNH_4SO_4 crystals*

The NMR spectra of the ^{1}H nuclei in KNH_4SO_4 were measured as a function of the temperature. One of the obtained spectra is shown in the inset of figure 4. We studied the recovery traces of the magnetization for ^{1}H and found that the inversion recovery traces of the ^{1}H ($I = 1/2$) nuclei can be

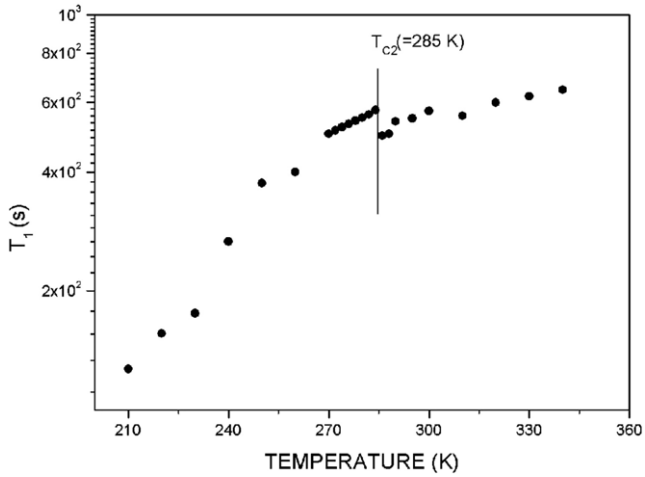

Figure 3. Temperature dependence of the spin–lattice relaxation time, T_1, for ^{7}Li in $LiNH_4SO_4$ crystals.

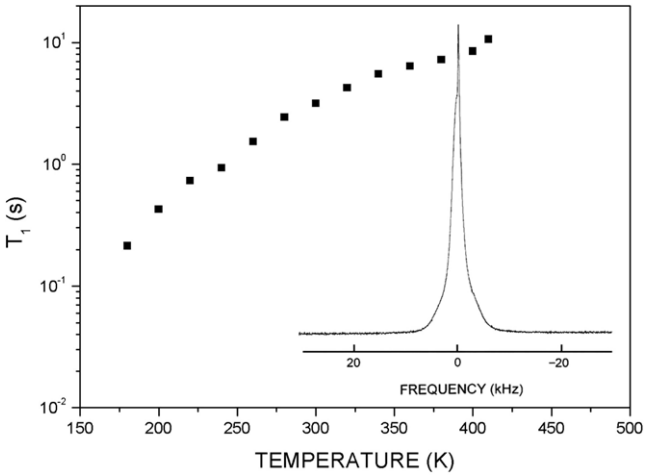

Figure 4. Temperature dependence of the spin–lattice relaxation time, T_1, for ^{1}H in KNH_4SO_4 crystals.

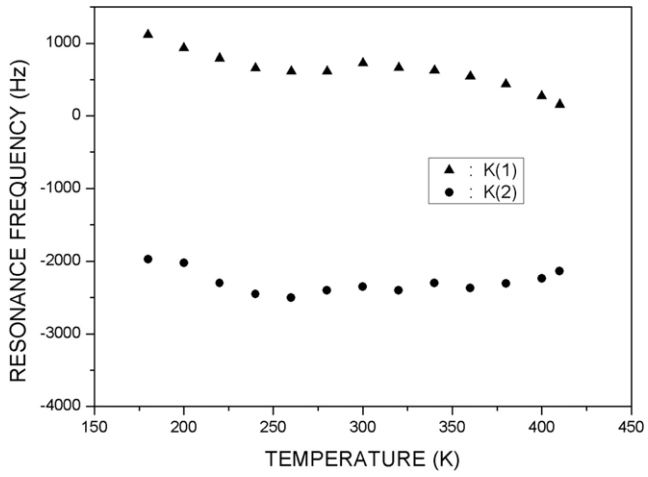

Figure 5. Splitting of the K(1) and K(2) resonance lines in KNH_4SO_4 crystals as a function of the temperature.

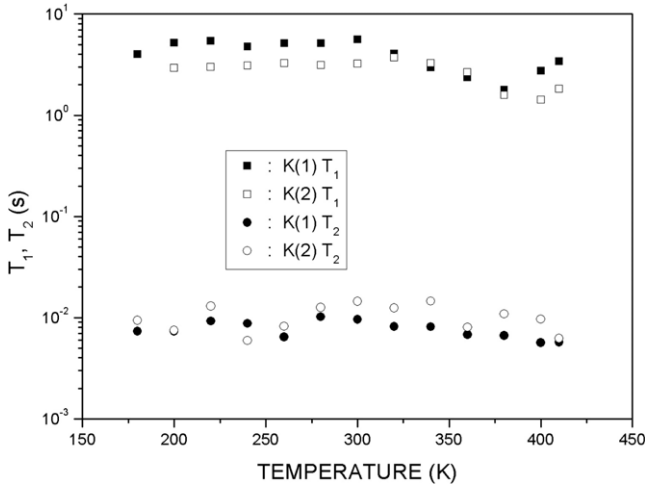

Figure 6. Temperature dependences of the spin–lattice relaxation times, T_1, and the spin–spin relaxation times, T_2, for K(1) and K(2) in KNH_4SO_4 crystals (inset: K(1) and K(2) NMR spectra for KNH_4SO_4).

represented by a single exponential function. The ^{1}H spin–lattice relaxation times were determined by fitting the recovery patterns to equation (1). The temperature dependence of T_1 for the ^{1}H nuclei is shown in figure 4. The relaxation times of the ^{1}H nuclei do not undergo significant changes in the temperature range between 180 and 410 K, which suggests that there are no phase transitions within this temperature range. The spin–lattice relaxation times were found to increase with increasing temperature.

The ^{39}K NMR spectrum consists of a pair of satellite lines and a central line. When the crystal is rotated about the crystallographic axis, crystallographically equivalent nuclei give rise to three lines, that is, a central line and two satellite lines. Two resonance lines instead of three resonance lines are obtained for the ^{39}K nucleus in the KNH_4SO_4 crystals at all the studied temperatures. The variations of the ^{39}K spectrum with temperature at the Larmor frequency 18.67 MHz are shown in figure 5. The resonance lines of ^{39}K were observed when the magnetic field was applied along an arbitrary direction. The magnitudes of the quadrupole parameters of the ^{39}K nuclei are of the order of megahertz; thus, usually only a central line is obtained. The satellite lines for ^{39}K nucleus, which correspond to the transitions $(-3/2 \leftrightarrow -1/2)$ and $(+1/2 \leftrightarrow +3/2)$, are out of range. Two resonance lines are obtained for the central transition of the ^{39}K NMR spectrum. This result points to the presence of two types of crystallographically inequivalent ^{39}K nuclei, namely K(1) and K(2). Small variations in the positions of the ^{39}K resonance lines are observed over the temperature range 180–420 K. These changes in the line positions indicate that the EFG tensor at the ^{39}K sites varies with temperature. This result thus suggests that the coordination geometry of the ^{39}K environment is displaced.

The ^{39}K spin–lattice relaxation times were measured using the saturation recovery method. We found that the recovery traces for the central resonance line of ^{39}K, with dominant quadrupole relaxation, can be represented by the combination of two exponential functions in equation (2). The spin–lattice relaxation time was obtained by inversion of the W_1 and W_2 values in equation (2): $[2(W_1 + 4W_2)]/5$. The temperature

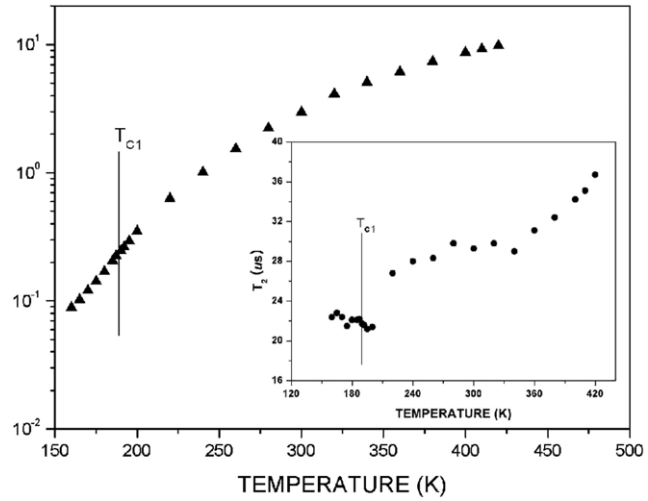

Figure 7. Temperature dependence of the spin–lattice relaxation time, T_1, for ^{1}H in $RbNH_4SO_4$ crystals (inset: ^{1}H spin–spin relaxation time for $RbNH_4SO_4$).

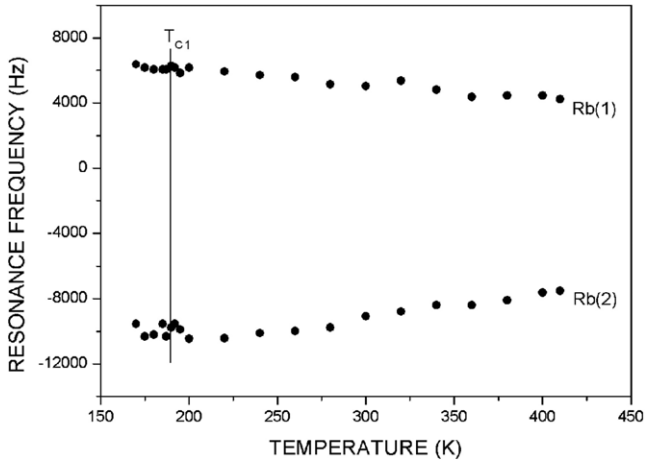

Figure 8. Splitting of the Rb(1) and Rb(2) resonance lines in $RbNH_4SO_4$ crystals as a function of the temperature.

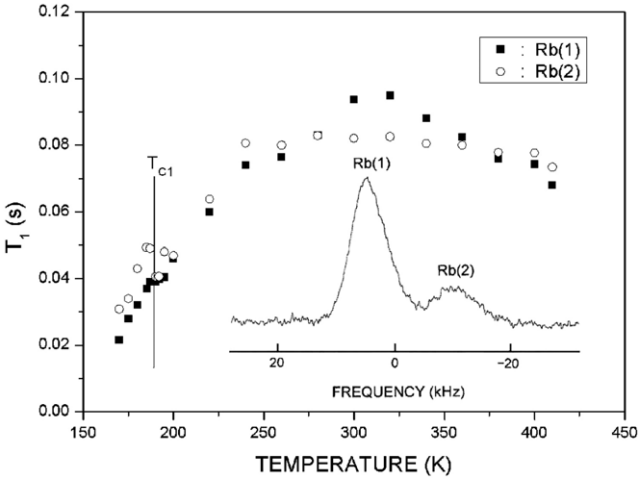

Figure 9. Temperature dependences of the spin–lattice relaxation times, T_1, for Rb(1) and Rb(2) in $RbNH_4SO_4$ crystals.

dependences of T_1 and T_2 for the K(1) and K(2) nuclei are shown in figure 6. The T_1 values obtained for the two resonance lines are the same within experimental error. The spin–lattice relaxation times of the ^{39}K nuclei were found to be nearly independent of the temperature. Moreover, they did not undergo any significant changes within the investigated temperature range, which indicates that no phase transitions occur within this temperature range. The T_2 values of the order of 10^{-2} s remained nearly constant upon increasing the temperature.

3.3. ^{1}H and ^{87}Rb NMR in $RbNH_4SO_4$ crystals

The NMR spectra for the ^{1}H nuclei in $RbNH_4SO_4$ were measured as a function of temperature. The ^{1}H spin–lattice relaxation times were obtained by using the inversion recovery method. The magnetizations for ^{1}H in this crystal were measured over a wide temperature range. Here, the relaxation times were determined from the intensities of the signals. The relaxation time, T_1, was determined directly from the slope of a plot of $\ln[(S(\infty) - S(t))/2S(\infty)]$ versus time t. The recovery trace can be satisfactorily fitted to a single exponential function, such as that in equation (1). The temperature dependence of T_1 for ^{1}H in a single crystal of $RbNH_4SO_4$ is shown in figure 7. As can be seen, the relaxation time did not show any abrupt changes within the temperature range of 160–420 K. The T_1 for the ^{1}H nucleus is more or less continuous at T_{C1} (=189 K). The ^{1}H spin–spin relaxation time, T_2, was determined by using the spin echo method. Near T_{C1}, this parameter increased abruptly, which is indicative of a phase transition. Although the T_1 values obtained for ^{1}H provide no evidence of a phase transition at T_{C1}, the T_2 values of the ^{1}H nuclei change at this temperature.

The ^{87}Rb NMR spectrum of crystalline $RbNH_4SO_4$ was obtained at a frequency of $\omega_o/2\pi = 130.93$ MHz when the magnetic field was applied along an arbitrary direction. When a crystal with crystallographically equivalent nuclei is rotated about its crystallographic axis, the nuclei give rise to three lines, that is, a central line and two satellite lines. Instead of three resonance lines for the ^{87}Rb nucleus, only two were obtained. The magnitudes of the quadrupole parameters of the ^{87}Rb nuclei are of the order of megahertz; thus, usually only a central line is obtained. Two resonance lines are obtained for the central transitions of Rb(1) and Rb(2). These two resonance lines are associated with two physically inequivalent nuclei, namely, Rb(1) and Rb(2). The positions of the ^{87}Rb resonance lines vary slightly over the temperature range 170–420 K as shown in figure 8. Thus, the quadrupole parameters of the two types of ^{87}Rb nuclei differ from each other. The central transition was found to decrease with increasing temperature. However, the changes in the central line were larger for Rb(2) than for Rb(1).

The ^{87}Rb spin–lattice relaxation times were measured using the saturation recovery method for the central resonance lines of the Rb(1) and Rb(2) nuclei. The stronger and weaker signals shown in the inset of figure 9 correspond to the central transition lines for Rb(1) and Rb(2), respectively.

The magnetizations for the ^{87}Rb nuclei were measured at several temperatures. The recovery traces for the central resonance lines of Rb with dominant quadrupole relaxation can be expressed as combinations of two exponential functions, as in equation (2). Here, the slope of a plot of log $[(S(\infty) - S(t))/S(\infty)]$ versus time t is not linear because the traces are combinations of two exponential functions. The temperature dependences of the ^{87}Rb relaxation rates W_1 and W_2 obtained from equation (2) show a similar trend with increasing temperature. In general, W_1 is less than W_2 at all temperatures. The temperature dependences of T_1 for the Rb(1) and Rb(2) nuclei in this single crystal are shown in figure 9. Near T_{C1}, T_1 for Rb(2) was found to undergo significant changes, whereas T_1 for Rb(1) remained more or less continuous. Abrupt changes in the relaxation times are associated with structural phase transitions. Therefore, the Rb(2) nucleus plays a major role at the phase-transition temperature. This result is consistent with the larger shift observed for the central line of Rb(2) than for that of Rb(1). The relaxation times T_1 increase with increasing temperature up to room temperature and then start to decrease.

4. Discussion and conclusions

ANH_4SO_4 (A = Li, K and Rb) single crystals were grown using the slow evaporation method. The spectra, the spin–lattice relaxation times and the spin–spin relaxation times of the ^{1}H, ^{7}Li, ^{39}K and ^{87}Rb nuclei in these three types of single crystals were investigated as a function of temperature using an FT NMR spectrometer. The NMR observations provided a consistent description of the dynamics of the studied nuclei in these materials. The T_1 of the ^{1}H nuclei in $LiNH_4SO_4$ crystals was found to exhibit significant changes near T_{C3} (=133 K), but showed an almost continuous trend at T_{C4} (=26 K). On the other hand, the ^{7}Li relaxation behavior varied abruptly at temperatures around T_{C2} (=285 K), which is indicative of a change in the state of the internal motion. This result indicates that the orthorhombic to monoclinic phase transition is a first-order phase transition. In the case of KNH_4SO_4, the relaxation times of the ^{1}H and ^{39}K nuclei do not change significantly between 180 and 410 K, suggesting that there are no phase transitions within this temperature range. The spin–lattice relaxation time for the ^{1}H nucleus increases with increasing temperature, whereas that for the ^{39}K nucleus decreases. Lastly, although the results obtained for the ^{1}H relaxation times in $RbNH_4SO_4$ crystals provide no evidence of a phase transition at T_{C1} (=189 K), the ^{87}Rb relaxation times do change near this temperature, which means that the T_1 of the ^{1}H and ^{87}Rb nuclei are dependent on their local H and Rb environments. Thus, we suggest that a shift of the oxygen atoms from the sulfate groups located around the A atom as compared with the room-temperature structure may also play an important role in the phase transitions. These phase transitions are accompanied by slight rotations of the SO_4 ions and a slight distortion of the lattice in the neighborhood of the A ions.

We now compare the ^{1}H and A NMR results obtained for the different ANH_4SO_4 (A = Li, K and Rb) crystals. The phase-transition properties of these compounds vary from case to case, for example, the KNH_4SO_4 crystals do not undergo any phase transitions, whereas $LiNH_4SO_4$ (T_{C4} = 27 K, T_{C4} = 133 K, T_{C4} = 284.5 K and T_{C4} = 459.5 K) and $RbNH_4SO_4$ (T_{C2} = 120 K and T_{C1} = 189 K) undergo successive phase transitions. The T_1 values for the ^{1}H nuclei are similar in all three crystals within the same temperature range; the ^{1}H spin–lattice relaxation times increase with increasing temperature. However, as the radii of the metal ions increase, a corresponding decrease in the spin–lattice relaxation times of the A nuclei is observed. The T_1 values for the ^{39}K and ^{87}Rb nuclei are about 10^0–10^2 and 10^{-1}–10^{-2} s, respectively, whereas that for the ^{7}Li nucleus is much longer, namely 10^2–10^3 s. The differences observed in the spin–lattice relaxation times of the A nuclei upon changing the alkali-metal ion may be related to the ionic radius and the lengths of the A–O bonds, as shown in table 1. This result suggests that the differences in the chemical properties of A (=Li, K and Rb) are responsible for the variations in the phase-transition properties observed in the crystals studied. Thus, although the three crystals have similar sulfate structures, their relaxation times exhibit different temperature dependences, which indicates that the three compounds undergo different phase-transition mechanisms. Therefore, it seems that the occurrence of phase transitions in these materials essentially depends on the presence of the metal ions.

Acknowledgment

This work was supported by the Korea Research Foundation Grant funded by the Korea Government (MOEHRD, Basic Research Promotion Fund) (KRF-2007-531-C00022).

References

[1] Aleksandrov K S, Aleksandrova I P, Anistratov A T and Shabanov V E 1977 *Izv. Akad. Nauk SSSr Ser. Fiz.* **41** 599
[2] Aleksandrova I P, Kabanov I S, Melnikova S V, Chekmasova T I and Yuzvak V I 1977 *Sov. Phys.—Solid State* **19** 605
[3] Stadnyk V Y and Romanyuk M O 1997 *Ferroelectrics* **192** 203
[4] Mitsui T, Oka T, Shiroishi Y, Takashige M, Iio K and Sawada S 1975 *J. Phys. Soc. Japan* **39** 845
[5] Shimizu H, Oguri A, Yasuda N and Fujimoto S 1978 *J. Phys. Soc. Japan* **45** 565
[6] Dollase W A 1969 *Acta Crystallogr.* B **25** 2298
[7] Itoh K, Ishikura H and Nakamura E 1981 *Acta Crystallogr.* B **37** 664
[8] Kruglik A I, Zinenko V I and Simonov M A 1978 *Ferroelectrics* **21** 441
[9] Aleksandrova I P, Kabanov I S, Melnikova S V, Chekmasova T I and Yuzvak V I 1977 *Sov. Phys.—Crystallogr.* **22** 182
[10] Simonson T, Denoyer F and Moret R 1984 *J. Physique* **45** 1257
[11] Yu J T and Chou S Y 1990 *J. Phys. Chem. Solids* **51** 1255
[12] Martins A R M, Germano F A, Filho J M, Melo F E A and Moreira J E 1991 *Phys. Rev.* B **44** 6723
[13] Watton A, Reynhardt E C and Petch H E 1978 *J. Chem. Phys.* **69** 1263
[14] Rao Y S and Sunandana C S 1995 *Solid State Commun.* **94** 563
[15] Stadnik V I, Romanyuk N A, Brezvin R S and Kurlyak V Yu 1994 *Opt. Spectrosc.* **77** 746

[16] Romanyuk N A, Stadnik V I, Brezvin R S and Kardash V I 1996 *Crystallogr. Rep.* **41** 840
[17] Andriyevsky B, Trojanek W C, Stadnyk V, Tuzyak M, Romanyuk M and Kurlyak V 2007 *J. Phys. Chem. Solids* **68** 1892
[18] Abragam A 1961 *The Principles of Nuclear Magnetism Resonance* (Oxford: Oxford University Press)
[19] Igarashi M, Kitagawa H, Takahashi S, Yoshizak R and Abe Y 1992 *Z. Naturf.* a **47** 313
[20] van der Klink J J, Rytz D, Borsa F and Hochi U T 1983 *Phys. Rev.* B **27** 89
[21] Shenoy R K and Ramakrishna J 1980 *J. Phys. C: Solid State Phys.* **13** 5429
[22] Andrew E R and Tunstall D P 1961 *Proc. Phys. Soc. (London)* **78** 1
[23] Lim A R, Jung J K and Jeong S Y 2002 *J. Phys. Chem. Solids* **63** 625
[24] Lim A R, Han T J and Jeong S Y 1999 *Phys. Status Solidi* b **214** 375